

# Deformation behavior and joining of a $\text{MgF}_2$ optical ceramic

C. Lorenzo-Martin<sup>a</sup>, D. Singh<sup>b,\*</sup>, J. Johnson<sup>b</sup>, J.L. Routbort<sup>a</sup>

<sup>a</sup> Energy Systems Division, Argonne National Laboratory, Bldg. 212/E206, 9700 S. Cass Avenue, Argonne, IL 60439, USA

<sup>b</sup> Nuclear Engineering Division, Argonne National Laboratory, Argonne, IL 60439, USA

Available online 28 March 2007

## Abstract

Compressive deformation behavior of a polycrystalline magnesium fluoride ( $\text{MgF}_2$ ) ceramic was investigated at temperatures ranging from 760 to 830 °C in an argon atmosphere at strain rates between  $2 \times 10^{-6}$  and  $4 \times 10^{-5} \text{ s}^{-1}$ . Steady-state flow stresses increased with increasing strain rates and ranged between 2 and 38 MPa. Stress exponents of  $\approx 1.4 \pm 0.2$  were determined at temperatures  $> 760$  °C, indicative of a viscous diffusion-controlled deformation mechanism. Activation energy, determined from flow stress as a function of temperature, at a constant strain rate, was  $\approx 476 \pm 60 \text{ kJ/mol}$ . Self-joining by plastic deformation of  $\text{MgF}_2$  was demonstrated at 830 °C at a strain rate of  $5 \times 10^{-6} \text{ s}^{-1}$ . The joined samples were characterized by optical transmission measurements and their transmittivity was  $\approx 80\%$  of the unjoined sample in the 2.5–8  $\mu\text{m}$  wavelength range.

© 2007 Elsevier Ltd. All rights reserved.

**Keywords:** Magnesium fluoride; Optical properties; Creep

## 1. Introduction

Polycrystalline magnesium fluoride ( $\text{MgF}_2$ ) is almost transparent in the infrared (IR) wavelength regime (2–8  $\mu\text{m}$ ).<sup>1,2</sup> Due to this unique property,  $\text{MgF}_2$  has applications for IR windows and coatings in optical instruments, space vehicles, and frontal domes in heat-seeking missiles.<sup>1–3</sup> Magnesium fluoride is an excellent candidate for thermal lensing because it has one of lowest temperature dependent refractive index distortions.<sup>3</sup> As compared to IR transparent single crystals, polycrystalline  $\text{MgF}_2$  is relatively simple and inexpensive to fabricate. However, fabrication of complex shaped engineering components using polycrystalline  $\text{MgF}_2$  still remains a major challenge.

Polycrystalline  $\text{MgF}_2$  is fabricated using typical ceramic processing routes by hot-pressing magnesium fluoride powder in a die in a controlled environment.<sup>1</sup> This process allows fabrication of simple shapes. One approach that is being considered is to join multiple simple-shaped parts to produce a complex part. In this regard, development of a joining process for optical materials such as  $\text{MgF}_2$ , without degradation of optical characteristics, becomes important.

In the literature, self-joining of  $\text{MgF}_2$  has been demonstrated by a diffusion bonding process without an interlayer<sup>4</sup> or using

a lithium fluoride (LiF) interlayer.<sup>5</sup> Diffusion bonding entailed applying a thin film of LiF on the mating surfaces of the pieces being joined and maintaining a constant compressive stress for  $> 3 \text{ h}$  at 550–575 °C. Without any interlayer, diffusion bonding was accomplished by applying constant pressure at 800–830 °C for about 6 h<sup>4</sup>. Limitations of this process are two-fold: (a) long hold times at elevated temperatures which can result in grain growth and (b) use of an extraneous interface material. Both factors can cause degradation of the optical and mechanical properties of the joined component. Thus, plastic deformation, as discussed in this paper, presents an approach to self-joining  $\text{MgF}_2$  that precludes the limitations imposed by the diffusion bonding process.

High-temperature plastic deformation process has been demonstrated for joining various structural ceramics and composites.<sup>6–9</sup> The joining process requires heating the components to elevated temperatures and deforming them at a constant displacement rate such that total strains are typically  $< 10\%$ . The mechanism by which pore-free joints are obtained is due to the interpenetration of grains at the interface as the result of grain boundary sliding (GBS).<sup>6–9</sup> There are several attributes that make the plastic joining process attractive: (a) it requires no surface preparation or interlayer material, (b) permanent deformation is minimal, and (c) the process occurs at lower temperatures and for shorter times relative to the conventional diffusional bonding.<sup>10</sup> The interface formed by plastic deformation is indistinguishable from the bulk material.<sup>9</sup> This attribute

\* Corresponding author. Tel.: +1 630 252 5009; fax: +1 630 252 2785.  
E-mail address: [dsingh@anl.gov](mailto:dsingh@anl.gov) (D. Singh).

is particularly significant when optical properties are of concern as in the case of joining of polycrystalline  $\text{MgF}_2$ .

High-temperature deformation behavior of polycrystalline  $\text{MgF}_2$  has not been reported. Because of the importance of deformation in processing and fabrication of components, a study of high-temperature deformation behavior of a polycrystalline  $\text{MgF}_2$  ceramic was undertaken. In addition, self-joining of  $\text{MgF}_2$  using plastic deformation was explored, so that complex shaped parts could be fabricated by joining simple geometries. Finally, the quality of joined  $\text{MgF}_2$  components was established by microstructural and optical characterizations.

## 2. Experimental details

### 2.1. Polycrystalline magnesium fluoride

Polycrystalline magnesium fluoride samples were procured from a commercial source (Superconix Inc., Lake Elmo, MN). Samples were fabricated by hot-pressing  $\text{MgF}_2$  powders. As-received samples were  $10\text{ mm} \times 10\text{ mm} \times 40\text{ mm}$ . The density of as-received samples was determined by the Archimedes method. The microstructure of the sample was examined on the fracture surface using a Hitachi Model S-4700-II (Tokyo, Japan) field emission scanning electron microscope (FE-SEM). Grain size was measured by the standard linear intercept method.<sup>11</sup> Phase analysis was conducted by room-temperature X-ray diffraction (XRD) measurements using a Phillips X-ray diffractometer (Model X'PERT, Almelo, The Netherlands) with a  $\text{Cu K}\alpha_1$  radiation. Data acquisition was conducted using a step-scan program run at  $100\text{ s}^\circ$  with a step size of  $0.01^\circ$  over a  $2\theta$  range of  $20\text{--}75^\circ$ . In addition, stability of the  $\text{MgF}_2$  phase was characterized by conducting XRD analysis on samples that were deformed and compared with the as-received samples.

### 2.2. Deformation study and joining

For deformation and joining experiments, right parallelepiped specimens ( $\approx 3\text{ mm} \times 3\text{ mm} \times 5\text{ mm}$ ) were cut from as-received  $\text{MgF}_2$  samples using a low speed diamond saw. Surfaces were as-cut. Specimens were subjected to uniaxial compression, at a constant cross-head displacement rate on an Instron machine (Model 1125, Canton, MA) equipped with an atmosphere-controlled high-temperature furnace.<sup>9</sup> All deformation and joining tests were conducted in an argon atmosphere. The furnace chamber was flushed with argon atmosphere prior to joining or deformation. Deformation tests were conducted in the temperature range from  $760$  to  $830^\circ\text{C}$  at strain rates varying from  $2 \times 10^{-6}$  to  $4 \times 10^{-5}\text{ s}^{-1}$ . For joining tests, two samples of  $\text{MgF}_2$  were mated and compressed. To ensure plastic deformation of  $\text{MgF}_2$  during joining, strain rate and joining temperature were selected on the basis of results from the deformation study of  $\text{MgF}_2$ . The joining temperature selected was  $830^\circ\text{C}$  at a strain rate of  $5 \times 10^{-6}\text{ s}^{-1}$ . All joinings were completed within  $0.5\text{ h}$ . The total permanent strains introduced during the plastic joining process ranged from  $\approx 0.05$  to  $0.08$ .

Microstructure of the as-received and deformed samples was examined by transmission electron microscopy (TEM). TEM

foils were prepared by first sectioning thin slices using a diamond blade and then further thinning by mechanical polishing. Thereafter, samples were ion milled using a Gatan (Pleasanton, CA) Model 691 precision ion polishing system. TEM was conducted using a Phillips CM-200 electron microscope operating at  $200\text{ kV}$ .

After joining, samples were sectioned, polished, and the joint interface was examined using an SEM (Hitachi S-4700, Tokyo, Japan). In addition, efficacy of the joint was established by conducting optical transmission measurements on samples before and after joining. Optical transmission measurements were conducted using a Brucker (Billerica, MA) Vertex 70 Fourier Transform Infrared (FTIR) spectrometer running OPUS software. This spectrometer has a resolution of  $0.5\text{ cm}^{-1}$ . Prior to evaluating the optical transmission, sample surfaces were polished to a mirror finish and cleaned in acetone.

## 3. Results

The density of the as-received  $\text{MgF}_2$  measured by the Archimedes method was  $3.1\text{ g/cm}^3$ , which was approximately 98% of the theoretical density of  $\text{MgF}_2$  taken as  $3.17\text{ g/cm}^3$ .

Fig. 1 is a photomicrograph of a fractured surface of as-received  $\text{MgF}_2$ . The microstructure was uniform with an average grain size of  $0.1\text{--}0.2\text{ }\mu\text{m}$ . In addition, the fracture morphology was intergranular. Fig. 2 shows the XRD pattern of an as-received  $\text{MgF}_2$  sample for which the major peaks correspond to magnesium fluoride.

Fig. 3 shows the typical stress-strain behavior obtained during compressive deformation of polycrystalline  $\text{MgF}_2$  at different strain rates. Initially, the stress increases linearly (elastic regime) with applied strain followed by deviation from linearity, indicative of plastic deformation. With further increase in strain, a steady-state stress was reached which is referred to as the flow stress. However, at the highest strain rates such as  $1 \times 10^{-5}\text{ s}^{-1}$  at  $828^\circ\text{C}$  (Fig. 3), there was evidence of work hardening. In such situations, it was difficult to determine the appropriate steady-state flow stress. In addition, there was an increase in the flow stress at a given strain rate after some strain had accumulated

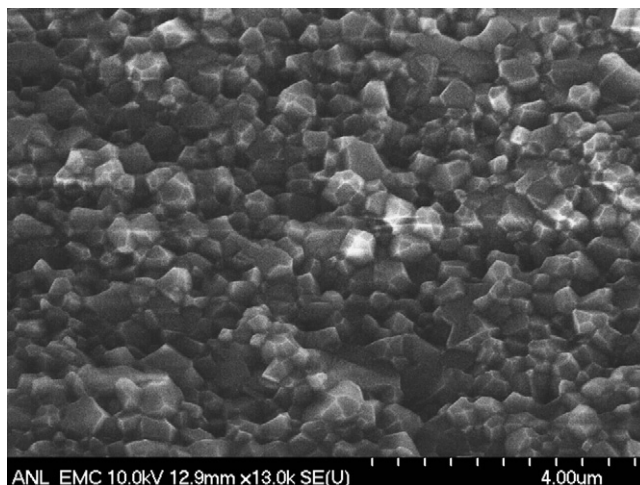


Fig. 1. Fracture surface of the as-received polycrystalline  $\text{MgF}_2$ .

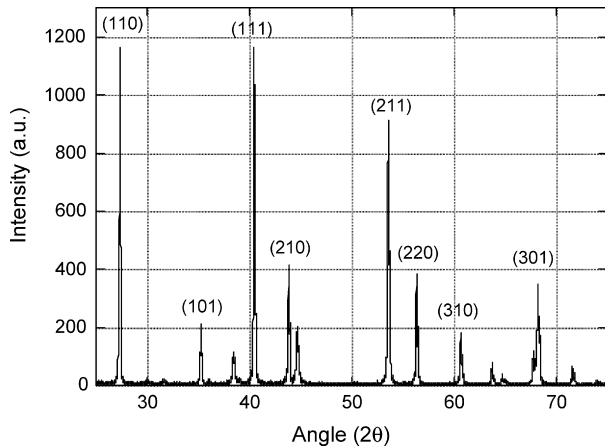


Fig. 2. X-ray diffraction pattern of as-received polycrystalline  $\text{MgF}_2$ .

(see tests conducted at  $5 \times 10^{-6} \text{ s}^{-1}$  in Fig. 3). This may be due to experimental uncertainties because of the low stresses. It is clear from Fig. 3 that the flow stresses increase with increasing applied strain rates at a constant test temperature. Similar stress-strain responses were obtained at other test temperatures.

Fig. 4 represents the strain-rate dependence of the flow stress on a log–log basis for the four temperatures investigated. If no microstructural changes occur during testing, a steady-state phenomenological creep equation can be used to define the dependence of strain rate on the flow stress<sup>12</sup>:

$$\dot{\epsilon} = A\sigma^n \exp(-Q/RT) \quad (1)$$

where  $\dot{\epsilon}$  is the strain rate,  $\sigma$  the flow stress,  $n$  is the stress exponent,  $A$  is a constant,  $Q$  the activation energy,  $R$  the gas constant, and  $T$  is the absolute test temperature. A stress exponent of  $n=1$  indicates that deformation process is diffusion-controlled.<sup>13</sup> Average value of  $n$ , estimated from best fits of the experimental data at the three test temperatures to Eq. (2), was  $1.4 \pm 0.2$ . For comparison, the bold line on Fig. 4 corresponds to  $n=1$ .

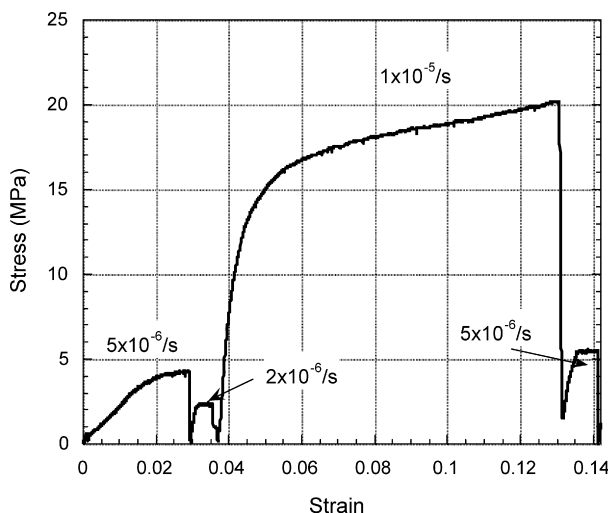


Fig. 3. Typical stress vs. strain behavior obtained during compressive deformation test performed at 828 °C on  $\text{MgF}_2$  at various strain rates.

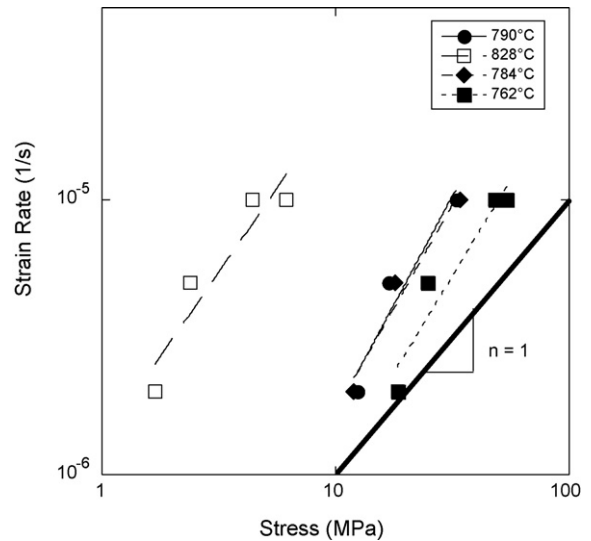


Fig. 4. Strain rate vs. steady-state stress behavior of polycrystalline  $\text{MgF}_2$  during compressive deformation at various temperatures.

At a constant strain rate, activation energy,  $Q$ , for the deformation process can be represented as

$$Q = nR \frac{\partial \ln \sigma}{\partial (1/T)} \quad (2)$$

Fig. 5 shows the Arrhenius plot of flow stress as a function of reciprocal absolute temperature at the three different strain rates tested. Activation energy determined, from the slopes of the various lines, was  $476 \pm 60 \text{ kJ/mol}$ . It is assumed that the stress exponent,  $n$ , was constant over the temperature range and a value of  $n=1.4$  was used for the calculation.

Fig. 6(a) and (b) are TEM micrographs of as-fabricated and 790 °C deformed (total deformation  $\approx 0.2$ )  $\text{MgF}_2$  samples, respectively. There was no cavitation observed at the grain boundaries. No discernible changes in the grain shape were

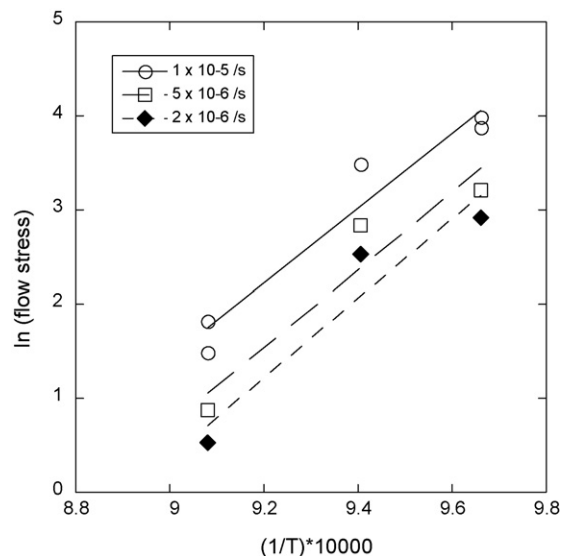


Fig. 5. Variation of flow stresses as a function of temperature for the strain rates tested in polycrystalline  $\text{MgF}_2$ .

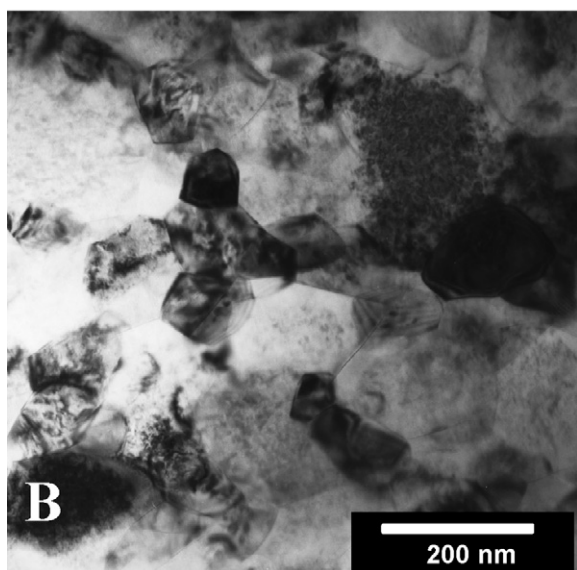
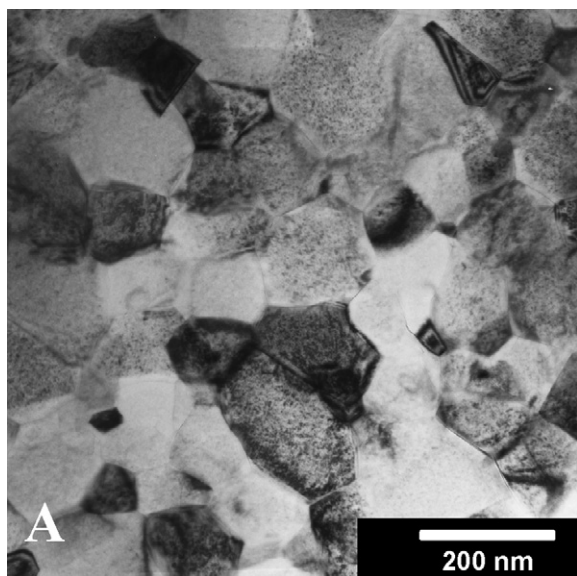


Fig. 6. TEM micrographs of polycrystalline  $\text{MgF}_2$ : (A) as-received and (B) post-deformation ( $790^\circ\text{C}$ , exposure time = 4.5 h, total  $\varepsilon \approx 20\%$ ).

observed. In addition, no dislocation networks were seen in the deformed sample.

Fig. 7 is a typical stress-strain plot obtained during joining of two pieces of  $\text{MgF}_2$  at  $830^\circ\text{C}$  and a strain rate of  $5 \times 10^{-5} \text{ s}^{-1}$ . The stress increased monotonically up to  $\approx 2 \text{ MPa}$ ; thereafter, it deviated from linearity, indicating plastic flow of the material. Typically, the cumulative deformation was  $\approx 0.07$  before samples were unloaded.

Fig. 8 shows an SEM image of the area in the vicinity of the joint. Location of the interface is shown by the arrows but is indistinguishable from the bulk  $\text{MgF}_2$ . Sample was not etched to reveal the grain structure.

Fig. 9 compares the optical transmission between the joined polycrystalline  $\text{MgF}_2$  and the unjoined sample. Optical transmissions were compared over the wavelengths ranging from 2.5 to  $8 \mu\text{m}$ . At wavelengths  $> 5 \mu\text{m}$ , joined samples have a transmittance behavior similar (within 95%) to the as-received sample.

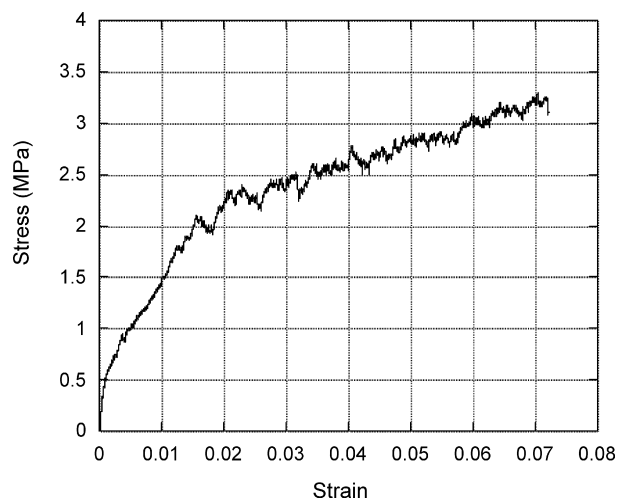


Fig. 7. Typical stress-strain profile obtained during joining of polycrystalline  $\text{MgF}_2$  by plastic deformation.

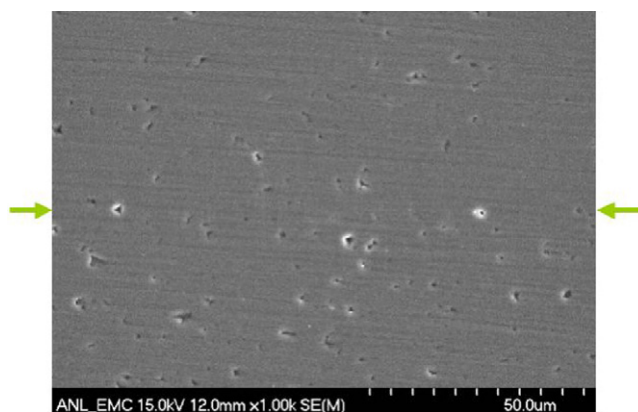


Fig. 8. Scanning electron micrographs of  $\text{MgF}_2$  sample joined at  $830^\circ\text{C}$  at  $5 \times 10^{-5} \text{ s}^{-1}$  strain rate; arrows indicate the joint interface.

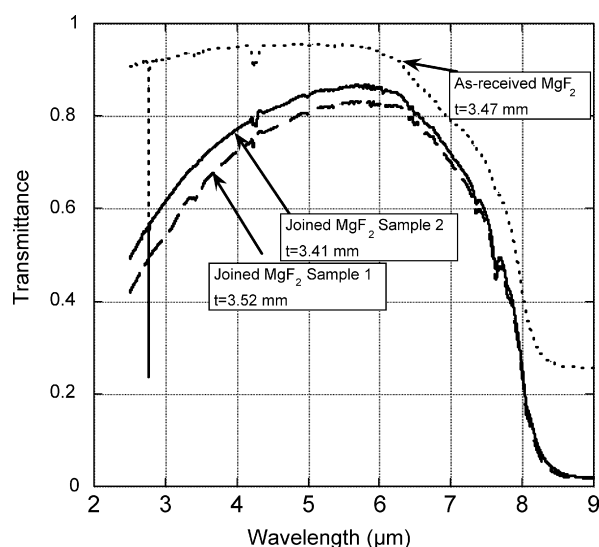


Fig. 9. Optical transmission of the joined polycrystalline  $\text{MgF}_2$  compared with the as-received monolithic  $\text{MgF}_2$ .



However, at wavelengths  $<5\text{ }\mu\text{m}$ , the discrepancy in the optical transmission of the joined and unjoined samples was larger. Relative areas under the transmission curves, over the entire wavelength range, provide a quantitative comparison of the optical transmission. It was determined that the samples joined by plastic deformation were approximately 80% as efficient as the monolithic sample. It should be noted that there are minor differences in the sample thicknesses, as listed in Fig. 9, along the optical path that were ignored.

#### 4. Discussion

Fine-grained polycrystalline ceramics<sup>14,15</sup> such as  $\text{Al}_2\text{O}_3$  and 3Y-TZP are known to plastically deform at elevated temperatures by grain boundary sliding (GBS). Grain boundary sliding is accommodated by a diffusion process.<sup>14,16</sup> Fine-grain structure assists in accommodating the local strains that are generated during GBS. Without this strain accommodation, the material will cavitate.<sup>13</sup> Evidence of grains rotation during GBS has been recently documented<sup>17</sup> in fine-grained  $\text{SrTiO}_3$ . It is believed that polycrystalline ceramics that exhibit GBS during deformation and concurrent grain rotation are excellent candidate materials for joining via the plastic deformation process.<sup>17</sup>

Based on the deformation behavior of polycrystalline  $\text{MgF}_2$  obtained in this study, it appears that the deformation behavior was a diffusion-assisted GBS mechanism. Deformation tests conducted at temperatures  $>760^\circ\text{C}$  and strain rates between  $2 \times 10^{-6}$  and  $1 \times 10^{-5}\text{ s}^{-1}$ , yielded a stress exponent value of 1.4; indicative of a diffusion-controlled deformation process.<sup>13</sup> Furthermore, as shown in TEM images of a deformed sample (Fig. 6), there was no evidence of cavitation and any deformation-induced dislocation structures. Also, no discernible changes in the grain shape and size were observed between the deformed and undeformed polycrystalline  $\text{MgF}_2$  (Fig. 6). These observations are consistent with the GBS as the deformation mechanism.

Activation energy of the diffusion-assisted deformation process can identify the slowest moving specie or the rate controlling process. The activation energy for deformation of  $\text{MgF}_2$  ceramic was  $476 \pm 60\text{ kJ/mol}$  determined from the Arrhenius plot of Fig. 5. Per the authors' knowledge there are no known values of deformation or self-diffusion activation energies for poly or single-crystalline  $\text{MgF}_2$  reported in the literature.  $\text{MgF}_2$  and  $\text{TiO}_2$  both have a tetragonal (rutile) structure with coordination number of 6 for cation and 3 for the anion.<sup>18</sup> Additionally, the ratio of cation to anion radii is about the same in  $\text{MgF}_2$  and  $\text{TiO}_2$ . Deformation and diffusion data exist for the  $\text{TiO}_2$  in the literature. It should be stated that comparing an oxide with the fluoride neglects any chemical effects that could be important. Polycrystalline rutile has been crept in four-point bending from 1100 to  $1200^\circ\text{C}$  by Philpot, et al.<sup>19</sup> They found that the strain rate was linearly proportional to the stress with a threshold stress. The creep rate also depended on the grain size and the oxygen partial pressure. They measured both undoped and 1% Ta doped  $\text{TiO}_2$  and reported activation energies of 264 kJ/mol for the undoped and 510 kJ/mol for the doped rutile. Activation energies of  $\text{MgF}_2$  and doped  $\text{TiO}_2$  are quite similar on a normal-

ized ( $Q/RT_m$ ) basis, where,  $T_m$  is the absolute melting point. This implies that doping affects the activation energy in  $\text{TiO}_2$  and possibly in  $\text{MgF}_2$ .

This study demonstrated that polycrystalline  $\text{MgF}_2$  ceramics can be successfully self-joined using plastic deformation. Microstructurally there was no discernible difference between regions along the interface and regions away from the interface. As indicated by the arrows in Fig. 8, no additional surface residual interfacial porosity was observed.

Optical transmission measurements further attest to the efficacy of the joint produced by plastic deformation. As shown in Fig. 9, the transmission spectrum as a function of wavelength was typical<sup>2</sup> of a polycrystalline  $\text{MgF}_2$ . The sharp external absorption peak at  $2.75\text{ }\mu\text{m}$  corresponds to that of water.<sup>2</sup> Joining by plastic deformation was approximately 80% as efficient (determined from area under the curve) as the transmittance of the as-received samples over the IR wavelength range from 2.5 to  $8\text{ }\mu\text{m}$ . This is in agreement with the 85% optical transmittance reported by Yen et al.<sup>4</sup> for a pure diffusional joint without an LiF interlayer. Clearly, at longer wavelengths ( $>5\text{ }\mu\text{m}$ ), the transmission behavior of the joined samples is much closer to the as-received sample. However, the discrepancy is quite large at wavelengths  $<5\text{ }\mu\text{m}$ . At shorter wavelengths, transmission losses are attributed to scattering of incident radiation from subsurface micropores.<sup>2</sup> The presence of some residual porosity is expected at the joint interface that contributed to the observed experimental discrepancy. It should be noted that limited joinings were made in this study and there was no process optimization. It is believed that by further process control, the discrepancy between the optical transmission behavior of joined and as-fabricated samples can be further reduced.

Change in grain size can significantly affect the optical transmittance in polycrystalline  $\text{MgF}_2$ . Lin et al.<sup>20</sup> found that there is an inverse relationship between grain size and optical transmission. Moreover, the effect is more profound at shorter wavelengths  $0.7\text{--}3\text{ }\mu\text{m}$  as opposed to longer wavelengths ( $>5.5\text{ }\mu\text{m}$ ). At a wavelength of  $2.5\text{ }\mu\text{m}$ , transmittance decreased by approximately 12% as the grain size increases from 0.5 to  $1.0\text{ }\mu\text{m}$ . Although, the TEM micrograph (Fig. 6) of post-deformed  $\text{MgF}_2$  sample does not show any grain size increase, this effect cannot be entirely discounted. A systematic study on the changes of grain in  $\text{MgF}_2$  during plastic deformation joining and its correlation to the optical transmittance needs to be conducted.

Finally, elevated temperature structural stability is an issue for halides, especially decomposition of fluorides. In this regard, X-ray diffraction was conducted on joined  $\text{MgF}_2$  samples and compared to the diffraction pattern of the as-received sample (Fig. 2). No difference was observed, indicating that the material was stable, within the resolution of the XRD, during the entire joining process (temperature and time).

#### 5. Conclusions

A compressive deformation study was conducted on a polycrystalline  $\text{MgF}_2$  optical ceramic in the temperature range from 760 to  $830^\circ\text{C}$  using strain rates of  $2 \times 10^{-6}$  to  $4 \times 10^{-5}\text{ s}^{-1}$ .

Steady-state plastic flow behavior was observed in this material and was attributed to a viscous diffusion-controlled mechanism. Activation energy of the deformation process was  $\approx 476$  kJ/mol and was comparable, on a normalized basis, to that observed for creep in doped  $\text{TiO}_2$ . Microstructural evidence indicated that the probable deformation mechanism was diffusion-assisted grain boundary sliding. Self-joining of  $\text{MgF}_2$  was demonstrated by plastic deformation at  $830^\circ\text{C}$  at a strain rate of  $5 \times 10^{-6} \text{ s}^{-1}$ . The resulting joined samples were characterized for transmittance by FT-IR measurements and were found to be  $\approx 80\%$  as efficient as the unjoined  $\text{MgF}_2$  in the IR wavelength range.

## Acknowledgments

This work was supported by the Office of FreedomCar and Vehicle Technologies of the U.S. Department of Energy, under Contract No. DE-AC02-06CH11357 at Argonne National Laboratory managed by UChicago Argonne, LLC. Authors acknowledge Drs. Xiao-Min Lin and John Schlueter for their assistance in conducting the FTIR measurements. The electron microscopy work was performed at the Electron Microscopy Collaborative Research Center at the Argonne National Laboratory.

## References

1. Buckner, D. A., Hafner, H. C. and Kreidl, N. J., Hot-pressing magnesium fluoride. *J. Am. Ceram. Soc.*, 1962, **45**, 435–438.
2. Chang, C. S., Hon, M. H. and Yang, S. J., The optical properties of hot-pressed magnesium fluoride and single-crystal magnesium fluoride in the 0.1 to  $9.0 \mu\text{m}$  range. *J. Mater. Sci.*, 1991, **26**, 1627–1630.
3. Dodge, M. J., Refractive properties of magnesium fluoride. *Appl. Opt.*, 1984, **23**(12), 1980–1984.
4. Yen, T. Y., Chang, Y. H., Yu, D. L., Yen, F. S., Tsai, D. S. and I.N. Lin, I. N., Diffusion bonding of  $\text{MgF}_2$  optical ceramics. *Mater. Sci. Eng.*, 1991, **A147**, 121–128.
5. Yen, T. Y., Chang, Y. H., Tsai, D. S., Duh, S. L. and Yang, S. J., LiF-film-assisted diffusion bonding of  $\text{MgF}_2$  ceramics. *Mater. Sci. Eng.*, 1992, **A154**, 215–221.
6. Ye, J. and Domínguez-Rodríguez, A., Joining of Y-TZP parts. *Scripta Metall. Mater.*, 1995, **33**, 441–446.
7. Gutiérrez-Mora, F., Domínguez-Rodríguez, A., Routbort, J. L., Chaim, R. and Guiberteau, F., Joining of yttria-tetragonal stabilized zirconia polycrystals using nanocrystals. *Scripta Mater.*, 1999, **41**, 455–460.
8. Goretta, K. C., Gutierrez-Mora, F., Picciolo, J. J. and Routbort, J. L., Joining alumina/zirconia ceramics. *Mater. Sci. Eng.*, 2003, **A341**, 158–162.
9. Singh, D., Gutiérrez-Mora, F., Chen, N., Goretta, K. C. and Routbort, J. L., Joining of advanced materials by plastic deformation. *Ceram. Eng. Sci.*, 2004, **25**(2), 113–119.
10. Scott, C. and Tran, V. B., Diffusion bonding of ceramics. *Am. Ceram. Bull.*, 1985, 29.
11. Underwood, E. E., *Quantitative Stereology*. Addison-Wesley Pub. Co, Reading, MA, USA, 1970.
12. Bretheau, T., Castaing, J., Rabier, J. and Veyssiere, P., Dislocation motion and high-temperature plasticity of binary and ternary oxides. *Adv. Phys.*, 1979, **28**, 835.
13. Langdon, T. G., The characteristics of superplastic-like flow in ceramics. In *Plastic Deformation of Ceramics*, ed. R. C. Bradt, C. A. Brookes and J. L. Routbort. Plenum Press, New York, 1985, pp. 251–268.
14. Xue, L. A. and Chen, I. W., Deformation and grain growth of low-temperature-sintered high-purity alumina. *J. Am. Ceram. Soc.*, 1990, **72**, 3518–3520.
15. Wakai, F., Sakaguchi, S. and Matsuno, Y., Superplasticity of yttria-stabilized tetragonal zirconia. *Adv. Ceram. Mater.*, 1986, **1**, 259.
16. Chokshi, A. H., Mukherjee, A. K. and Langdon, T. G., Superplasticity in advanced materials. *Mater. Sci. Eng. R*, 1993, **10**, 237–241.
17. Singh, D., Lorenzo-Martin, M., Chen, G., Gutiérrez-Mora, F. and Routbort, J. L., High-temperature deformation behavior in  $\text{SrTiO}_3$  ceramics. *J. Eur. Ceram. Soc.*, 2007, **27**, 3377–3384.
18. Shannon, R. D., *Acta Crystallogr.*, 1976, **A32**, 751–757.
19. Philpot, K. A., Ikuma, Y., Miller, G. R. and Gordon, R. S., High-temperature steady-state creep of polycrystalline rutile, pure and doped with tantalum. *J. Mater. Sci.*, 1983, **18**, 1698–1708.
20. Lin, W. Y., Hon, M. H. and Yang, S. J., Effect of grain growth on hot-pressed optical magnesium fluoride ceramics. *J. Am. Ceram. Soc.*, 1988, **71**(3), C136–C137.